Simões *et al. Cellular & Molecular Biology Letters* (2026) 31:92
https://doi.org/10.1186/s11658-026-00926-8

Cellular & Molecular Biology Letters

BRIEF REPORT Open Access

High-temperature ssBP-LAMP breaks the barrier of nonspecific amplification and unlocks the full potential of LAMP diagnostics

Rita S. Simões[1,2,3], Pedro Bule[2,3], Carlos M. G. A. Fontes[1,2,3] and João S. Teodoro[1*]

*Correspondence:
João S. Teodoro
joao.teodoro@nzytech.com
[1]NZYtech—Genes and Enzymes, Campus do Lumiar, Building J, 1649-038 Lisbon, Portugal
[2]CIISA—Centre for Interdisciplinary Research in Animal Health, Faculty of Veterinary Medicine, University of Lisbon, 1300-477, Lisbon, Portugal
[3]Associate Laboratory for Animal and Veterinary Sciences (AL4AnimalS), 1300-477, Lisbon, Portugal

Abstract

Background Loop-mediated isothermal amplification (LAMP) is a highly attractive nucleic acid detection method for decentralized molecular diagnostics, but its broader adoption has been limited by unpredictable nonspecific amplification (NSA). Here, we dissect the fundamental determinants of LAMP specificity and present a new high-temperature ssBP-LAMP technique to suppress NSA without compromising assay sensitivity or speed.

Methods Ubiquitous bioinformatic tools for prediction and design of primer sets and their characteristics were employed to generate a panel of 21 primer sets targeting diverse bacterial, viral, fungal, and human targets. Fluorometric ssBP-LAMP was implemented with a series of coordinated modifications, from increased temperature (only possible owing to a novel, engineered thermostable strand displacement Bst polymerase enzyme) to fine-tuning of additives and auxiliary enzymes. Finally, proof-of-concept validation using both fluorometric and colorimetric approaches for ssBP-LAMP was performed, and their resistance to common inhibitors of molecular diagnostics was evaluated.

Results We show for the first time that primer design alone is insufficient to ensure specificity, and bioinformatic predictions are insufficient predictors of efficiency and, more importantly, of specificity, even when using elevated reaction temperatures. This suggests that NSA frequently originates during the thermal ramp-up phase, before the assay reaches its operational temperature. To address this, we employed a thermolabile single-stranded DNA-binding protein (ssBP) from bacteriophage T7, which transiently sequesters primers during temperature ramp-up. When combined with conventional LAMP primers and elevated assay temperatures (≥ 68 °C), ssBP consistently suppressed NSA across all tested targets. This approach translated directly to both liquid and lyophilized master mixes, enabling highly specific ssBP-LAMP detection by real-time fluorescence and colorimetry. These formulations retained robust sensitivity (down to 10–100 copies/reaction for real-time detection), eliminated false positives, and exhibited tolerance to clinically relevant inhibitors such as plasma, hemoglobin, saliva, and urine, especially in real-time fluorescence detection.

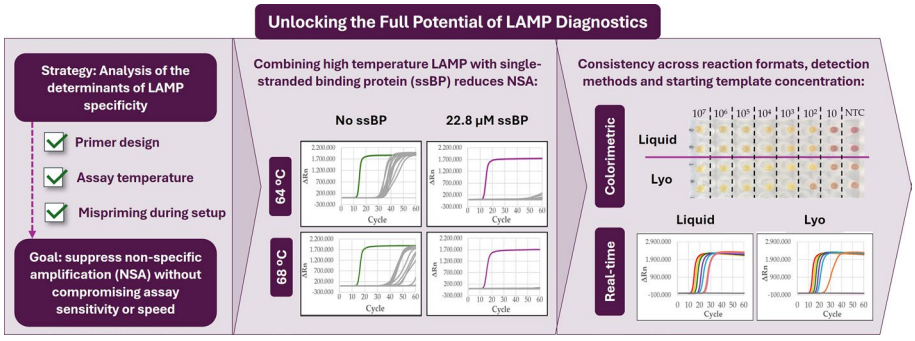
Conclusions Together, the results establish high-temperature ssBP-LAMP as a rapid (< 15 min), specific, inhibitor-tolerant, and highly adaptable molecular diagnostic

© The Author(s) 2026. **Open Access** This article is licensed under a Creative Commons Attribution-NonCommercial-NoDerivatives 4.0 International License, which permits any non-commercial use, sharing, distribution and reproduction in any medium or format, as long as you give appropriate credit to the original author(s) and the source, provide a link to the Creative Commons licence, and indicate if you modified the licensed material. You do not have permission under this licence to share adapted material derived from this article or parts of it. The images or other third party material in this article are included in the article's Creative Commons licence, unless indicated otherwise in a credit line to the material. If material is not included in the article's Creative Commons licence and your intended use is not permitted by statutory regulation or exceeds the permitted use, you will need to obtain permission directly from the copyright holder. To view a copy of this licence, visit http://creativecommons.org/licenses/by-nc-nd/4.0/.

technology that overcomes key limitations of conventional LAMP while achieving analytical performance comparable to qPCR, with broad relevance for both clinical and point-of-care testing.

Keywords Loop-mediated isothermal amplification, LAMP, Bst polymerases, Nonspecific amplification, Primer design, Colorimetric LAMP

Graphical Abstract



Background

The advent of the polymerase chain reaction (PCR) by Mullis and colleagues [1, 2] revolutionized nucleic acid detection, catalyzing the development of a large diversity of amplification-based diagnostic strategies. Although quantitative PCR (qPCR) is the current gold-standard technique in molecular diagnostics, its long time to result combined with the inherent requirement of specialized reagents, equipment, and trained personnel makes it a rather demanding diagnostic tool [3, 4], limiting its accessibility in decentralized or point-of-care (POC) settings.

In recent decades, the development of isothermal amplification protocols has provided novel opportunities toward more accessible, cost-effective, and faster molecular tests. Among these, loop-mediated isothermal amplification (LAMP) has gained prominence for its ability to amplify DNA with speed and simplicity, operating under a constant temperature, using a strand-displacing polymerase and a complex but elegant primer system of either four or six oligonucleotides [5, 6]. The inclusion of an additional loop primer pair was shown to accelerate reaction kinetics, reducing the time to result (TTR) to as little as 5 min, which makes LAMP especially attractive for resource-limited and point-of-care (POC) applications [6, 7].

Despite growing interest, broader diagnostic adoption of LAMP has been hampered by several technical challenges. A key limitation lies in its susceptibility to nonspecific amplification (NSA), which can lead to false positive results, particularly under suboptimal primer design or assay conditions [8–10]. This susceptibility stems from the inherent complexity of LAMP reactions: using multiple primers at high concentrations while operating at relatively low stringency temperatures can result in intra- and interprimer interactions that bypass the intended target. Hence, optimizing primer design is central not only for reaction efficiency but also to ensure specificity. While some design principles are borrowed from qPCR, such as balanced GC content and appropriate melting temperatures, LAMP primers require additional considerations, especially regarding their length, thermodynamics, and spacing [11, 12]. For example, inner primers (FIP and BIP) typically span 38–42 nucleotides, whereas outer and loop primers are shorter, and

the Gibbs free energy (ΔG) of primer ends must be carefully tuned to avoid dimer formation [5, 7, 13].

In addition to primer design, different approaches have been explored to improve LAMP accuracy, particularly by increasing reaction specificity. For example, additives such as betaine or tetramethylammonium chloride can suppress nonspecific binding, although not without trade-offs in enzyme activity or reaction kinetics [10, 14]. Guanidine hydrochloride is also known to accelerate LAMP reactions and improve target sensitivity [15], although its effects are not consistent across all primer sets or sample matrices, suggesting incomplete mechanistic understanding. More recently, we proposed that increasing LAMP reaction temperature could reduce the formation of spurious primer–primer interactions. However, the conventional Bst polymerase displays limited thermostability under such conditions [16]. To address this, we screened a panel of naturally occurring Bst-like enzymes and identified three novel candidates capable of supporting LAMP amplification at temperatures up to 72 °C while maintaining resistance to common qPCR inhibitors, as the specific impact of high-temperature LAMP on the suppression of NSA remains to be systematically evaluated [16]. Finally, a wide array of LAMP detection formats has been developed to suit a range of diagnostic applications, ranging from real-time LAMP detection using fluorescence to more elaborate formats like lateral flow and end-point methods detecting reaction turbidity and pH-sensitive colorimetric shifts [17]. While these approaches offer different balances between simplicity, sensitivity, and quantification, many LAMP assays still struggle with consistency, particularly when applied to diverse targets or deployed in point-of-care environments.

In this study, we set out to address the persistent challenges that limit the broader adoption of LAMP as a diagnostic tool, namely the unpredictability of primer performance, the prevalence of nonspecific amplification, and the limited robustness in complex sample matrices. We designed a diverse panel of targets and primer sets, rigorously analyzed their performance under high stringency conditions, and dissected the role of thermodynamics and pre-amplification dynamics in controlling assay specificity. Building on these insights, we developed and tested four LAMP master mixes, real-time and colorimetric, liquid and lyophilized, tailored for laboratory and point-of-care applications, and evaluated their tolerance to clinically relevant inhibitors. Together, these advances establish a cohesive and generalizable framework that transforms high-temperature LAMP (≥68 °C) into a predictable, robust, and widely deployable diagnostic platform.

Materials and methods

LAMP primer design and sequences

To ensure broad relevance and technical robustness, all primers were selected from well-validated literature sources [18–23] (Supplementary Table S1) or designed using the NEB® LAMP Primer Design Tool version 1.4.0 (New England Biolabs, Ipswich, MA; https://lamp.neb.com/) and ordered from Integrated DNA Technologies, Inc (IDTDNA, Coralville, IA). All primer sequences are provided in Supplementary Table S2. The melting temperatures, guanine–cytosine (GC) content, and Gibbs free energy (ΔG) of designed primers were determined using the OligoAnalyzer™ tool (IDTDNA; https://www.idtdna.com/calc/analyzer) by selecting the following parameter settings: 50 mM

Na^+, 8 mM Mg^{++}, and 1.4 mM dNTPs. Regarding the fourth parameter that needs to be defined in this tool, oligonucleotide concentration, FIP and BIP primers were used at 1.6 μM, F3 and B3 primers at 0.2 μM, and FL and BL primers at 0.4 μM. Unless otherwise specified, all LAMP reactions throughout this study were performed using primers at the concentrations described above.

DNA templates

The template DNAs used in this study were synthetic DNA fragments produced in-house (NZYtech, Lisbon, Portugal), which were quantified using a NanoDrop One spectrophotometer (Thermo-Fisher, Waltham, MA) and diluted in IDTE 1× TE solution pH 8.0 (IDTDNA) to obtain serial DNA concentrations ranging from 10^7 to 10 copies/μL. The only exception was the single-strand DNA of the M13 bacteriophage, which was obtained from New England Biolabs. The DNA sequences of all targets evaluated in the assays described in this study are as follows (accession no.: position in the DNA sequence): the breast cancer 1 (*BRCA1*) gene from *Homo sapiens* (NG_005905.2: 9258–9424), the maltose B (*malB*) gene from *Escherichia coli* (J01648.1: 3243–3388), the envelope (*E*) gene from severe acute respiratory syndrome coronavirus 2 (SARS-CoV-2) (NC_045512.2: 26,245–26,472), the nucleocapsid (*N2*) gene from SARS-CoV-2 (NC_045512.2: 28,274–29,533), the pyruvate:ferredoxin oxidoreductase domain (PFO domain) gene from *Candida auris* (NC_072813.1: 774–947), the preprotein translocase (*SecY*) gene from *Leptospira interrogans* (EU358000.1: 401–611), the β subunit of the bacterial RNA polymerase (*rpoB*) gene from *Mycobacterium tuberculosis* (CP089779.1: 3,492,186–3,495,704), the 28S ribosomal RNA (28S rRNA) gene from *Candida albicans* (NW_139715.1: 2081–3180), and the fibrinogen-binding protein B (*FbsB*) gene from *Streptococcus agalatidae* (CP010874.1: 831,317–833,412).

Strains, plasmids, molecular cloning, expression, and purification of ssBP

Escherichia coli strains used for gene cloning (DH5-Alpha) and expression (BL21 (DE3)) were provided by NZYtech. For DNA extraction and purification, the NZYMiniprep kit was employed (NZYtech). The gene encoding the single-stranded DNA-binding protein (ssBP) of *Escherichia* phage T7 (NC_001604.1: 9158–9856) was synthesized (NZYtech) and cloned into the prokaryotic pHTP1 expression vector (NZYtech), which led to the incorporation of two poly-histidine (6xHis) sequences (N- and C-terminal) that allowed subsequent recombinant protein purification by immobilized metal ion affinity chromatography (IMAC). The molecular cloning was performed through the ligation independent cloning (LIC)-based method using the NZYEasy Cloning & Expression kit I (NZYtech). Positive clones were analyzed by DNA sequencing through Macrogen Europe CES service (Amsterdam, The Netherlands) to confirm the correct sequence insertion and integrity. The recombinant enzyme was expressed in *E. coli* BL21(DE3) grown in 250 mL of NZY Auto-Induction LB medium (NZYtech) and purified via IMAC resorting to ÄKTA go™ protein purification system (Cytiva, Wilmington, DE). Cells were collected through centrifugation, chemically lysed in NZY Bacterial Cell Lysis Buffer (NZYtech), and purified according to standard protocol. The protein's relative solubility, expression levels and estimated molecular weight were confirmed by sodium dodecyl sulfate (SDS)-polyacrylamide gel electrophoresis (PAGE) (NZYtech). Gels were imaged using a Gel Doc XR+ System (Bio-Rad, Hercules, CA). Since the molecular weight

determined by SDS was slightly higher than estimated (Supplementary Fig. S1) [24, 25], a functional test was also conducted following protocols established in-house before the use of ssBP in the experiments described in this study.

Reagents

The reagents used in the preparation of the inhibitors' bank tested were the following: bile salts, human hemoglobin, human serum, and human plasma were all acquired from Sigma-Aldrich (Sigma-Aldrich, St. Louis, MO); ethanol was obtained from PanReac AppliChem (Barcelona, Spain), and human saliva and urine were obtained from Innovative Research (Novi, MI). For protein electrophoresis, standard 14% SDS gels were prepared in-house using NZYtech's acrylamide/bis-acrylamide. Cresol Red used in colorimetric assays was from Sigma-Aldrich. All other reagents not listed were of the highest degree of purity commercially available.

LAMP primer set testing

The 21 primer sets designed for the 10 targets were characterized regarding isothermal amplification following established protocols in a real-time LAMP setup utilizing StepOnePlus™ Real-Time PCR System (Thermo-Fisher). A typical LAMP reaction comprised 1× Polaris® BstY Reaction Buffer 10×, 6 mM Polaris® $MgSO_4$, 1.4 mM Polaris® dNTPs mix, 1× NZY LAMP Fluorescent dye 50× (NZYtech), 2.5 µL 10× LAMP Primer Mix (16 µM FIP, 16 µM BIP, 2 µM F3, 2 µM B3, 4 µM LoopF, 4 µM LoopB), 8 U Polaris® Glycerol-free BstY Polymerase 80 U/µL, 10^5 copies of template DNA, and water up to 25 µL. Unless otherwise specified, LAMP assays were conducted at 69 °C.

Analysis of the effect of increasing reaction temperature and ssBP incorporation

For these particular experiments, real-time LAMP assays were performed to amplify eight targets from various origins: the *BRCA1* gene from *H. sapiens*, the *malB* gene from *E. coli*, the *E* gene from SARS-CoV-2, the *N2* gene from SARS-CoV-2, the *IV* gene from Enterobacteria phage M13, the PFO domain gene from *C. auris*, the *SecY* gene from *L. interrogans*, and the *rpoB* gene from *M. tuberculosis*. Isothermal amplification was performed in a real-time LAMP setup using the StepOnePlus™ Real-Time PCR System (Applied Biosystems). Reactions were carried out as specified above in a final volume of 25 µL, with amplification performed at 64 and 68 °C in the presence of increasing concentrations of single-stranded DNA-binding protein (ssBP): 0, 11.4, and 22.8 µM.

LAMP master mixes

Two master mixes were prepared to assess the sensitivity of different LAMP detection methods: the Colorimetric LAMP Master Mix 4× and the Real-time LAMP Master Mix 4×. The Colorimetric LAMP Master Mix 4× is a mixture of 4× Polaris® BstY Reaction Buffer 10×, 0.5 mM Cresol Red, 5.6 mM Polaris® dNTP mix 25 mM, IVD (NZYtech), 1.28 U Polaris® Glycerol-free BstY Polymerase 80 U/µL (NZYtech), and 92.8 µM ssBP. The Real-time LAMP Master Mix 4× consists of 4× Polaris® BstY Reaction Buffer 10×, 5.6 mM Polaris® dNTP mix 25 mM, IVD (NZYtech), 1.28 U of Polaris® Glycerol-free BstY Polymerase 80 U/µL (NZYtech), and 92.8 µM ssBP.

Lyophilization (freeze-drying)

Each master mix was gently homogenized by using a vortex mixer at a low speed to avoid introducing bubbles and prevent any adverse effects on the lyophilization process. The master mixes were dispensed into suitable glass lyophilization vials (660 µL/vial), which were then spun before slow freezing at −20 °C to favor adequate ice crystal formation. The frozen aliquots were then transferred to a lyophilizer, and the following protocol was applied:

Stage	Duration (h)	Temperature (°C)	Ramp	Pressure
Primary freezing	4	−40	N/A	Atmospheric
Primary drying, first stage	2	−45	0.3 °C/ min	70 mTorr
Primary drying, second stage	24	−40	0.3 °C/ min	70 mTorr
Secondary drying	4	+25	0.3 °C/ min	70 mTorr

Upon freeze-drying completion, the vacuum was broken with an inert gas (N_2) to avoid the introduction of water vapor before sealing the vials with rubber stoppers.

Assessment of detection sensitivity

The Colorimetric LAMP Master Mix 4× and the Real-time LAMP Master Mix 4× prepared as previously detailed were assessed for their ability to amplify multiple starting template DNA concentrations following established protocols. A typical colorimetric LAMP reaction (25 µL) comprised 1× Colorimetric LAMP Master Mix 4×, 2.5 µL 10× LAMP Primer Mix (as above), 1 µL template DNA, and water up to 25 µL. A typical real-time LAMP reaction (25 µL) comprised 1× Real-time LAMP Master Mix 4×, 6 mM Polaris® $MgSO_4$ 100 mM (NZYtech), 1× NZY LAMP Fluorescent dye 50× (NZYtech), 2.5 µL 10× LAMP Primer Mix (as above), 1 µL template DNA, and water up to 25 µL. The templates used in these assays were synthetic DNA fragments corresponding to various targets: the *BRCA1* gene from *H. sapiens*, the *malB* gene from *E. coli*, the *E* gene from SARS-CoV-2, the *N2* gene from SARS-CoV-2, the *IV* gene from Enterobacteria phage M13, the PFO domain gene from *C. auris*, the *SecY* gene from *L. interrogans*, the *rpoB* gene from *M. tuberculosis*, and the *28S rRNA* gene from *C. albicans.*

Evaluation of inhibitor resistance

The Colorimetric LAMP Master Mix 4× and Real-time LAMP Master Mix 4× were tested for their resistance to common qPCR inhibitors following established protocols. A typical colorimetric LAMP reaction (25 µL) comprised 1× Colorimetric LAMP Master Mix 4×, 2.5 µL 10× LAMP Primer Mix (as above), 10 µL inhibitor, 1 µL template DNA, and water up to 25 µL. A typical real-time LAMP reaction (25 µL) comprised 1× Real-time LAMP Master Mix 4×, 6 mM Polaris® $MgSO_4$ 100 mM (NZYtech), 1× NZY LAMP Fluorescent dye 50× (NZYtech), 2.5 µL 10× LAMP Primer Mix (as above), 10 µL inhibitor, 1 µL template DNA, and water up to 25 µL. The template DNA used in these assays was a synthetic DNA fragment corresponding to 10^5 copies/µL of the *E* gene sequence of SARS-CoV-2.

Template copy number calculation

The following equation was used to determine the number of copies of template DNA for each case:

$$\#\text{copies of DNA template per}\,\mu L = \frac{\text{DNA concentration}\,(\text{ng}/\mu L) \times 6.022 \times 10^{23}}{\text{Length of template}\,(\text{bp}) \times 10^{9} \times 650}$$

Calculations were made on the basis of the assumption that the average molecular weight of a base pair (bp) is 0.65 kDa and using a conversion factor to nanograms (ng) of 1×10^9.

Preparation of spiked samples and extraction protocol

Escherichia coli (DH5-Alpha) cells (NZYtech) were grown in 200 mL LB Broth medium (NZYtech) to an OD_{600nm} of approximately 0.5, which is equivalent to a cell concentration of 4×10^8 cells/mL. At this point, cells were put on ice and used to prepare spikes for urine samples as well as for control samples (containing water instead of urine) to obtain a final collection of spiked samples with cell concentrations ranging between 1×10^8 cells/mL and 1×10^5 cells/mL. Extraction of DNA from the prepared spiked samples, both urine and control, was performed using the NZY Mag Blood & Tissue DNA Isolation Kit (NZYtech) and the TANBead Maelstrom™ Switch 8 (Taiwan Advanced Nanotech Inc, Taiwan). Extraction success was confirmed both by agarose gel and nanodrop quantification of the extracted samples.

Real-time assays for pathogen nucleic acid detection in spiked samples

The real-time LAMP assays performed to detect the *malB* gene (*E. coli*) in spiked urine and control samples were carried out using the Real-time LAMP Master Mix 4× prepared as previously detailed. A typical real-time LAMP reaction comprised 1× Real-time LAMP Master Mix 4×, 6 mM Polaris® $MgSO_4$ 100 mM (NZYtech), 1× NZY LAMP Fluorescent dye 50× (NZYtech), 2.5 µL 10× LAMP Primer Mix (as above), 2.5 µL sample, and water up to 25 µL. The real-time PCR assays performed to detect the *malB* gene (*E. coli*) in the spiked samples were conducted using the NZYSupreme qPCR Green Master Mix (SYBR Green qPCR) and the NZYSupreme qPCR Probe Master Mix (TaqMan qPCR), both provided by NZYtech. Real-time PCR assays using the SYBR detection method were prepared as follows: 1× NZYSupreme qPCR Green Master Mix, 10 µM Primer F3, 10 µM Primer B3, 2 µL sample, and water up to 20 µL. Real-time PCR assays using the probe detection method were prepared as follows: 1× NZYSupreme qPCR Probe Master Mix, 10 µM Primer F3, 10 µM Primer B3, 10 µM Probe (5′-/56-FAM/CCG ACA AAC/ZEN/ACC ACG AAT TCA CCT T/3IABkFQ/-3′), 2 µL ,sample and water up to 20 µL. All assays were performed in a StepOnePlus™ Real-Time PCR System (Thermo-Fisher) following the amplification protocols indicated by the manufacturer.

Statistical analysis

The experimental results are expressed as the mean of a series of replicates ($n \geq 3$) and standard deviation (SD). All statistical analyses were performed using Microsoft Excel® 2021 and GraphPad Prism (version 9.0.0).

Results

Establishing a diverse primer set panel for LAMP-based molecular diagnostics

Although guided by well-established principles, primer design for LAMP remains largely empirical. It is arguably the most critical determinant of assay success, particularly

under the rigorous conditions required for clinical diagnostics, where both sensitivity and specificity are crucial [26]. To explore the intrinsic determinants of LAMP primer performance, we assembled 21 distinct LAMP primer sets targeting different sequences in the genome of a wide array of living organisms by combining two approaches (Supplementary Table S1): (i) mining well-validated sequences from the literature and (ii) designing de novo candidates with the NEB LAMP Primer Design Tool (https://lamp.neb.com/#!/), which generates the six standard primers required for LAMP assays (conventionally named F3, B3, FIP, BIP, FL, and BL). These 21 primer sets (Supplementary Table S2) were then subjected to experimental evaluation under standardized assay conditions to assess whether LAMP performance and the prevalence of nonspecific amplification could be linked to primer design features.

Primer sets were generated using the tool's default parameters, with melting temperatures (Tm) optimized for high-temperature amplification: ~ 60 °C for the outer and inner primer regions (F3, B3, F2, and B2) and ~ 65 °C for the loop primers. Additional design constraints, such as primer length, GC content, interprimer spacing, and avoidance of secondary structures, were automatically enforced by the software to maximize amplification efficiency and specificity under isothermal conditions. The resulting primer sets, listed in Supplementary Table S2, span ten distinct biological systems of diagnostic and biomedical relevance, including viruses, bacteria, fungi, and a human genetic marker, reflecting the broad utility of modern molecular diagnostics [27]. Most targets were associated with two or three distinct primer sets, acknowledging the intrinsic variability in LAMP performance and the common occurrence of false positives in no-template controls (NTCs) [7, 28]. By combining established and newly designed primers across a diverse range of diagnostic contexts, this panel allowed for a rigorous and comprehensive assessment of primer-dependent variability in LAMP specificity and sensitivity.

Experimental assessment of LAMP primer set performance and specificity

Following the design and selection of 21 LAMP primer sets targeting a range of clinically and biologically relevant templates, we next sought to evaluate their experimental performance under identical reaction conditions. Each primer set was tested in standardized real-time LAMP assays at 69 °C using Polaris® BstY Polymerase 80 U/µL (NZYtech), a thermostable strand displacement DNA polymerase engineered for high-temperature LAMP reactions. Each assay was performed in triplicate with 10^5 copies of the corresponding target DNA and included nine NTC reactions to ensure a robust assessment of specificity and accuracy in the absence of target sequences. For SARS-CoV-2, an RNA virus, a synthetic DNA fragment encompassing the *E* and *N2* gene regions was used as the template.

Despite uniform reaction conditions, substantial variability was observed among primer sets, both in terms of amplification efficiency, measured as time to result (TTR), and specificity, assessed by the percentage of nonspecific amplification (%NSA) and time to NTC (TTN) (Table 1, Fig. 1). Product melting analysis [29] at the end of the real-time LAMP assays confirmed that NSA observed in NTC reactions with 11 primer sets was not a result of assay template contamination (data not shown). Several primer sets yielded high signal intensities with rapid TTR values (Fig. 1A–C).

By comparing amplification outcomes (TTR) with primer sequence parameters (Table S2) and self and cross-dimer ΔG (Supplementary Table S3), with data summarized in

Table 1 Overview of LAMP primer set performance and sequence parameters for 21 assays targeting diverse diagnostic organisms

Target	Set	Six primers			Four primers						
		TTR (min)	TTN (min)	%NSA	TTR (min)	TTN (min)	%NSA	T_m BIP_H	T_m FIP_H	Average ΔG	$\Delta G < -8$ count
Homo sapiens (*BRCA1* gene)	1	8.74	24.36	11.11	24.34	23.24	100.00	59.6	60.6	− 6.02	4
	2	14.60	NA	0.00	ND	ND	ND	59.6	63.1	− 5.85	2
Candida auris (*PFO domain* gene)	1	6.35	25.40	44.44	14.14	21.03	100.00	63.1	63.1	− 7.17	7
	2	5.37	20.96	100.00	14.09	17.53	100.00	63.0	63.5	− 6.43	5
Candida albicans (*28S rRNA* gene)	1	9.78	NA	0.00	ND	ND	ND	61.3	60.4	− 7.35	9
	2	6.85	NA	0.00	ND	ND	ND	64.2	63.3	− 7.21	6
	3	6.48	NA	0.00	ND	ND	ND	63.6	63.6	− 8.34	9
Escherichia coli (*malB* gene)	1	7.02	20.21	22.22	ND	ND	ND	63.7	63.8	− 6.72	6
	2	6.92	26.14	55.56	25.76	20.35	100.00	64.0	63.3	− 6.26	4
Leptospira interrogans (*SecY* gene)	1	11.75	NA	0.00	ND	ND	ND	61.0	61.0	− 7.12	8
	2	9.54	28.04	33.33	18.17	20.74	100.00	60.6	61.0	− 6.92	7
	3	27.3	NA	0.00	ND	ND	ND	49.4	61.3	− 5.53	0
S. agalatiae (*FbsB* gene)	1	6.09	24.15	100.00	16.65	27.04	22.22	60.0	60.1	− 7.65	6
Mycobacterium tuberculosis (*rpoB* gene)	1	11.28	26.00	22.22	16.93	20.09	77.78	63.8	66.5	− 7.56	9
	2	7.40	NA	0.00	ND	ND	ND	64.2	67.7	− 8.86	12
Hepatitis B virus (*P* gene)	1	5.36	19.50	100.00	12.67	18.66	100.00	63.4	64.3	− 7.05	7
	2	4.90	20.78	100.00	13.89	20.31	100.00	63.5	64.8	− 8.57	10
	3	8.84	24.58	77.78	18.69	23.76	88.88	67.1	59.9	− 6.03	3
SARS-CoV-2 (*E* gene)	1	7.39	NA	0.00	ND	ND	ND	60.7	60.6	− 6.92	6
SARS-CoV-2 (*N2* gene)	1	6.32	NA	0.00	ND	ND	ND	62.4	63.5	− 7.28	7
M13 bacteriophage (*IV* gene)	1	10.08	NA	0.00	ND	ND	ND	60.6	61.0	− 6.77	8

Time to result (TTR, in minutes) and percentage of nonspecific amplification (%NSA) were determined from real-time LAMP assays at 69 °C. The %NSA corresponds to the number of NTC reactions that exhibited amplification compared with the total number of NTC reactions [9] performed for each enzyme. For each primer set, the melting temperature (T_m, °C) of the hybridizing regions of the inner primers (FIP_H and BIP_H), the average T_m of outer (F3/B3) and loop (LF/LB) primers, the average free energy (ΔG, kcal/mol) across all self- and cross-primer interactions, and the number of strong interactions ($\Delta G < -8$ kcal/mol) are listed. NA = No amplification detected within 30 min. ND = Not determined

Table 1, several trends emerged. Amplification efficiency (TTR) was strongly correlated with the melting temperature of the hybridizing segments of the inner primers (FIP_H and BIP_H). Primer sets yielding rapid amplification (TTR < 7 min) consistently featured FIP_H/BIP_H regions with T_m values ≥ 63 °C. In contrast, delayed sets, such as *L. interrogans* set 3, exhibited hybridization regions with T_m values approaching or below 60 °C, indicating suboptimal annealing at 69 °C. These findings reinforce the critical role of inner primer thermodynamics in controlling LAMP kinetics at elevated temperatures [7, 30]. While the T_m of FIP_H/BIP_H segments ≥ 63 °C may generally predict faster TTR, primer–dimer ΔG values, target accessibility, and internal primer architecture may be important secondary contributors. For example, *S. agalactiae* set 1 illustrates how efficient template engagement may offset lower primer melting temperatures, leading to unexpectedly rapid amplification. Outer primers (F3/B3), which mediate the initial strand displacement, displayed broader T_m ranges and did not strongly correlate with amplification timing once loop cycling was initiated (Supplementary Table S2). Similarly, loop primers (LF/LB), whilst associated with improvements in amplification speed, were not consistent predictors of kinetic performance (Supplementary Table S2).

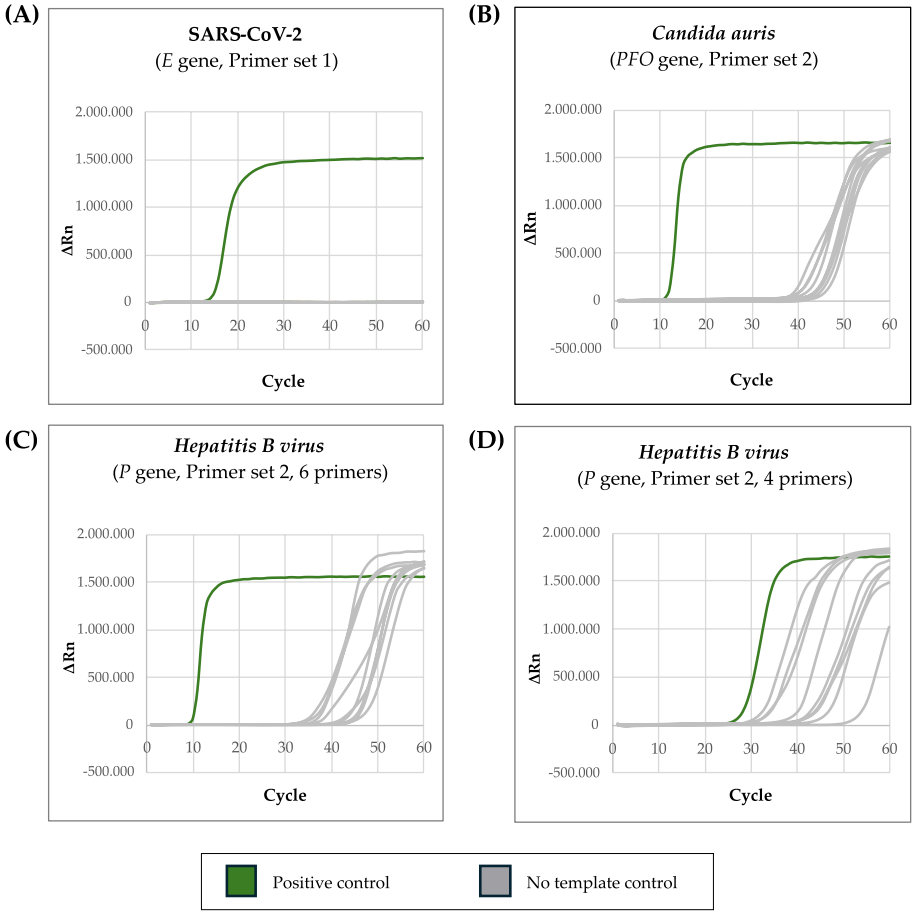


Fig. 1 Representative real-time LAMP amplification profiles selected from 21 primer sets tested. Amplification curves illustrate the performance of LAMP assays targeting three distinct sequences, conducted at 69 °C using 10^5 copies of template DNA per reaction. Each assay was performed in triplicate (green curve: average of three replicates) alongside nine no-template controls (NTCs; individual amplification curves in grey). **A**–**C** examples using full six-primer sets (FIP, BIP, F3, B3, FL, and BL), revealing differences in time to result (TTR) and levels of nonspecific amplification (NSA). **D** The same primer set as **C**, but in a four-primer format (without loop primers), illustrating the impact of loop primer exclusion on reaction kinetics and specificity. Each cycle represents 30 s, totaling 30 min for the full assay duration

To further assess factors that may contribute to delayed amplification, we analyzed the self-dimerization propensity of full-length primers (Supplementary Table S3). Although some variability in average self-dimer ΔG (across FIP, BIP, F3, B3, FL, and BL) was observed among functional sets, efficient amplification was observed even in the presence of strong self- and cross-dimer interactions. These findings challenge the criteria defined by primer design tools such as OligoAnalyzer™ (IDTDNA) which recommend a ΔG more positive than −9 kcal/mol to ensure that oligonucleotide performance is not impaired (Table 1). Collectively, these findings confirm that the hybridization thermodynamics of the inner primers, particularly the T_m of the FIP_H and BIP_H segments, are primary determinants of amplification efficiency. These data suggest that a minimum T_m threshold of ≥ 63 °C for these regions should be considered when designing LAMP assays intended to operate at or above 68 °C.

Unexpectedly, nonspecific amplification (%NSA) did not correlate with any single primer thermodynamic property, suggesting that existing metrics may be insufficient to predict assay specificity (Table 1). For example, primer sets with zero NSA, such as

M13 phage (gene *IV*), SARS-CoV-2 (gene *N*), and *C. albicans* set 2, presented average ΔG values as low as −8.34 kcal/mol and up to eight strong dimer interactions, indistinguishable from those in highly nonspecific sets. In addition to %NSA, we examined the time to amplification in no-template controls (TTN) to further dissect assay specificity. However, TTN values also varied widely among primer sets with comparable thermodynamic profiles. For example, *C. auris* set 1 exhibited a TTN of 25.4 min with 44.4% NSA, while *L. interrogans* set 2 had a TTN of 28.04 min but only 33.3% NSA. Conversely, sets such as *M. tuberculosis* set 2 and SARS-CoV-2 (*E* and *N2* genes) showed no NSA (0%) and no detectable NTC amplification within 30 min (TTN = NA), despite containing several strong dimer interactions.

To evaluate whether nonspecific amplification (%NSA) and time to amplification in no-template controls (TTN) could be mitigated by reducing the primer set from six to four primers, we retested ten primer sets that had previously exhibited NSA in the full six-primer configuration by omitting the loop primers. The comparative results are shown in Table 1 and exemplified in Fig. 1C, D. While omitting loop primers predictably resulted in delayed amplification, reflected in longer TTR values across all tested sets [28, 30], their exclusion had no consistent effect on reducing NSA or delaying TTN. In several instances, %NSA remained unchanged or only marginally decreased, and TTN values continued to overlap with amplification observed in the presence of target DNA. These results suggest that loop primers are unlikely to be the main contributors to the emergence of nonspecific amplifications. Instead, the data point toward the core primer sets, FIP/BIP and F3/B3, as the primary drivers of assay specificity. This observation also highlights the difficulty of predicting nonspecific amplification based solely on primer thermodynamics. Other variables, such as local template structure, primer-template accessibility, or even stochastic primer interactions, may also play a critical role in driving unspecific amplifications in LAMP assays.

High-temperature LAMP is still vulnerable to NSA: the role of pre-assay mispriming

The initial screening of 21 primer sets at 69 °C was designed to suppress nonspecific amplification (NSA), a well-documented challenge in LAMP diagnostics [16]. However, despite the elevated temperature, 11 of the 21 primer sets still yielded detectable amplification signals in no-template controls (Table 1), suggesting that increased thermal stringency is not, by itself, sufficient to universally prevent misamplification. To systematically evaluate how temperature modulates both specificity and reaction efficiency, we selected six representative primer sets, comprising both NSA-prone and NSA-free sets at 69 °C, and assayed them across a temperature range of 62–72 °C.

The results (Fig. 2) offer important mechanistic insights into how temperature modulates LAMP specificity. Notably, all LAMP assays were functional across the entire temperature range tested, except for *C. auris* set 1, which failed to produce amplification at 72 °C (Fig. 2A). This observation further underscores the broad operational range of Polaris® BstY polymerase and supports its suitability for high-temperature LAMP diagnostics (Fig. 2A). In terms of specificity, most primer sets exhibited elevated %NSA values and shorter TTNs at the lower end of the temperature spectrum (62–64 °C), indicating a higher tendency for nonspecific amplification under these conditions (Fig. 2B). For example, *H. sapiens* set 1 exhibited 100% NSA and TTNs below 15 min, while *E. coli*

(A)

	Time to result (minutes)					
	62 °C	64 °C	66 °C	68 °C	70 °C	72 °C
C. auris (*PFO* domain gene, Set 1)	5.18	5.04	5.33	5.97	8.47	NA
SARS-CoV-2 (*E* gene, Set 1)	5.07	4.94	4.96	5.47	7.67	27.38
SARS-CoV-2 (*N2* gene, Set 1)	6.32	5.46	4.95	4.81	5.40	14.70
H. sapiens (*BRCA1* gene, Set 1)	5.52	5.63	5.86	6.42	7.89	12.68
E. coli (*malB* gene, Set 1)	6.73	5.96	5.60	5.47	6.08	10.35
L. interrogans (*SecY* gene, Set 2)	6.94	6.45	6.25	6.35	7.78	15.14

(B)

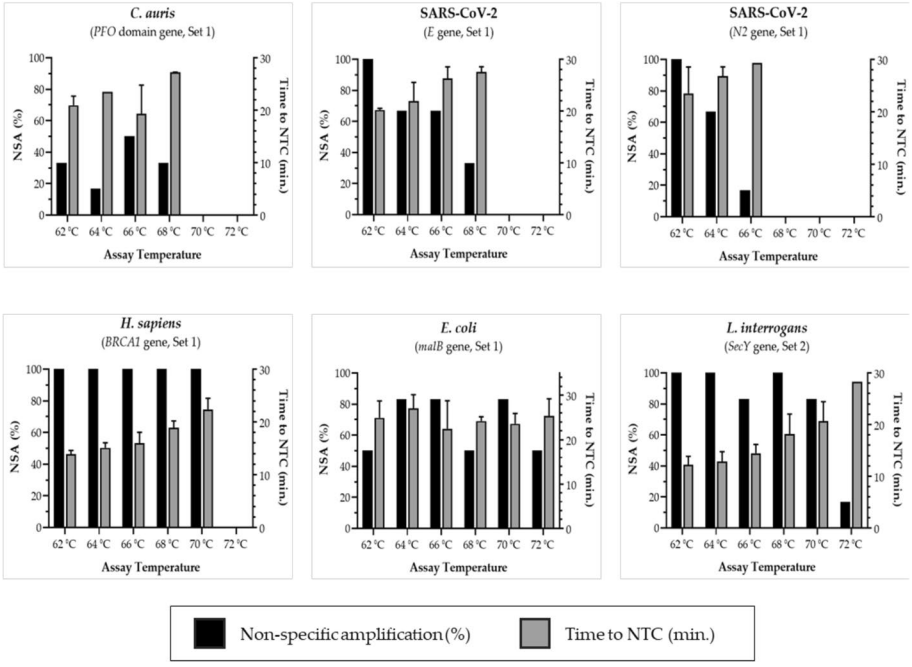


Fig. 2 Effect of assay temperature on **A** TTR and **B** nonspecific amplification (NSA) and time to amplification in no-template controls (TTN) for six representative LAMP primer sets. **A** lists the TTR for the six targets at the different amplification temperatures (62–72 °C) tested. **B** displays the percentage of reactions showing NSA (black bars, left *Y*-axis) and the mean TTN in minutes (gray bars, right *Y*-axis) at those same temperatures. Each plot corresponds to a different target and primer set, including *H. sapiens*, *C. auris*, *E. coli*, *L. interrogans*, and SARS-CoV-2 (E and N2). Error bars represent the standard deviation from replicates. NSA generally decreased with increasing temperature, while TTN increased

set 1 and *L. interrogans* set 2 also showed elevated NSA levels (> 80%) and early NTC amplification, indicating robust off-target priming at these temperatures.

As the reaction temperature increased, a gradual decline in NSA incidence and an increase in TTN were observed in most primer sets. Notably, the SARS-CoV-2 *E* and *N2* sets transitioned from nearly 100% NSA at 62–64 °C to 0% NSA at ≥ 68 °C, with TTNs extending beyond 25 min or remaining undetected. This transition strongly supports the role of elevated temperature in enhancing hybridization stringency and minimizing nonspecific interactions [16]. A comparable, albeit less dramatic, trend was observed for *C. auris* set 1, where NSA progressively declined and TTNs became more delayed as temperature increased. For the *H. sapiens* set 1, NSA was only fully suppressed at 72 °C; however, this was accompanied by reduced amplification kinetics, with TTR extending to 12 min at 72 °C from 5–6 min at lower temperatures. In contrast, *E. coli* set 1 and *L. interrogans* set 2 deviated from this trend. Both exhibited persistent NSA across all

temperatures, with %NSA remaining above 70% and TTNs remaining below 20 min even at 72 °C. These observations imply that NSA in these cases may not be driven solely by insufficient thermal stringency. Instead, they suggest a pivotal contribution from early-phase primer–primer or primer–template interactions that occur during the assay setup and pre-heating phase. Since Bst-family enzymes retain significant strand displacement activity even at suboptimal temperatures [31], amplification may be inadvertently initiated before the reaction mixture reaches the target temperature, rendering subsequent thermal correction ineffective.

Taken together, these results demonstrate that, while elevated temperatures enhance specificity by reducing NSA and extending TTN, this strategy is not universally effective in reducing LAMP nonspecific amplification in the context of molecular diagnostics. In primer sets prone to mispriming, the onset of NSA likely occurs during the assay assembly stage or the early heating phase, driven by transient, low-stringency hybridizations in the presence of an active polymerase. Thus, implementing strategies that delay amplification until the reaction mixture reaches the intended temperature may offer a robust solution to improve LAMP specificity in clinical and point-of-care applications.

Mitigation of nonspecific amplification by single-stranded DNA-binding protein

Building on the observation that elevated temperatures alone are insufficient to fully suppress NSA in certain primer sets, we next explored whether early stage mispriming events, occurring before the reaction reaches thermal equilibrium, might represent a key vulnerability in LAMP assays. To address this possibility, we employed thermolabile single-stranded DNA-binding proteins (ssBPs), known to transiently sequester single-stranded oligonucleotides and impede premature primer annealing and extension before denaturation [32–34]. These proteins typically dissociate from single-stranded oligonucleotides at ~ 45 °C, allowing amplification to commence only under optimal hybridization conditions.

To investigate the hypothesis that LAMP assays are susceptible to nonspecific primer interactions occurring during the pre-assay and temperature ramping phases, we cloned and expressed gene 2.5 protein (gp2.5) [35] from *Escherichia* phage T7 (UniProt P03696; PDB 1JE5) in *E. coli* and purified the protein to near homogeneity (Supplementary Fig. S1). We then evaluated the influence of ssBP on LAMP specificity and efficiency using eight representative primer sets previously tested at 69 °C. Each assay was conducted at 64 °C and 68 °C, in the presence of 0 µM (control), 11.4 µM, or 22.8 µM ssBP, corresponding, respectively, to 2.5-fold and fivefold molar excess of ssBP relative to the total primer concentration (4.4 µM). The results are summarized in Table 2 and exemplified in Fig. 3, with additional data displayed in Supplementary Fig. S2.

Across all tested primer sets, the addition of ssBP had a negligible impact on amplification speed of positive controls, with time to result (TTR) values remaining within ±1 min across the entire dataset (Table 2). This finding supports the notion that recombinant gp2.5 ssBP does not interfere with Polaris® BstY Polymerase activity or impede primer annealing once the reaction has initiated, consistent with its thermal dissociation above 45 °C. In contrast, ssBP exerted a marked effect on assay specificity given that at 22.8 µM, the protein consistently delayed or abolished amplification in no-template controls, as reflected by extended time-to-NTC (TTN) values and substantial reductions in the percentage of nonspecific amplification (%NSA) (Table 2; Fig. 3).

Table 2 Impact of single-stranded DNA-binding protein (ssBP) on LAMP amplification kinetics and specificity at 64 and 68 °C

[ssBP]	TTR (min)						TTN (min)						NSA (%)					
	64 °C			68 °C			64 °C			68 °C			64 °C			68 °C		
	0 µM	11.4 µM	22.8 µM	0 µM	11.4 µM	22.8 µM	0 µM	11.4 µM	22.8 µM	0 µM	11.4 µM	22.8 µM	0 µM	11.4 µM	22.8 µM	0 µM	11.4 µM	22.8 µM
H. sapiens BRCA1 Set 1	5.90	5.63	6.29	6.58	6.02	6.62	16.01	23.48	26.38	21.28	24.54	–	100	33.3	16.7	58.3	16.7	0.00
C. auris PFO Set 1	4.76	4.73	5.42	5.09	4.97	5.46	19.42	20.74	21.33	18.50	25.85	–	50.0	41.7	16.7	50.0	25.0	0.00
E. coli malB Set 1	6.42	6.01	6.85	5.9	5.34	5.81	21.42	18.76	23.58	22.86	18.49	25.39	83.3	100	91.7	100	100	83.3
L. interrogans SecY Set 2	6.56	5.99	5.25	6.24	5.63	4.57	13.30	21.35	27.87	22.10	20.45	–	100	75.0	9.10	100	41.7	0.00
M. tuberculosis rpoB Set 2	8.15	8.53	10.36	6.42	6.91	8.66	19.97	19.61	24.24	17.21	18.78	–	91.7	75.0	83.3	91.7	75.0	0.00
SARS-CoV-2 *E* Set 1	4.92	4.86	6.17	5.33	4.89	6.44	17.20	15.03	21.06	22.31	20.08	27.40	100	100	100	75.0	100	25.0
SARS-CoV-2 *N2* Set 1	5.64	5.85	7.70	5.30	4.82	6.45	21.44	24.56	27.41	11.80	28.57	–	50.0	33.3	50.0	8.33	8.33	0.00
M13 bacteriophage *IV* Set 1	6.69	4.36	4.73	7.52	4.05	4.33	24.19	23.48	25.49	–	26.23	–	25.0	100	41.7	0.00	8.33	0.00
Average	6.13	5.75	6.60	6.05	5.33	6.04	19.12	20.88	24.67	19.44	22.87	27.08	75.0	69.8	51.2	60.4	46.9	13.5

Eight LAMP primer sets were tested at two temperatures (64 and 68 °C) in the presence of 0, 11.4 or 22.8 µM ssBP. Amplification performance was evaluated by time to result (TTR, min), time-to-no-template control signal (TTN, min), and percentage of nonspecific amplification (%NSA). TTR values reflect amplification speed in the presence of target DNA. TTN values indicate the time at which amplification was detected in no-template controls, and %NSA represents the proportion of NTC replicates showing amplification within 30 min. Missing TTN values ("–") indicate no detectable signal during the assay. Average values across all sets are shown in the last row

For instance, in *H. sapiens* set 1 at 64 °C, %NSA dropped from 100% (0 μM ssBP) to 17% (22.8 μM ssBP), accompanied by a TTN increase from 16 to 26.4 min. At 68 °C, NSA was fully suppressed (%NSA = 0%), with no detectable NTC amplification within the 30-min assay window. Comparable improvements were observed in *C. auris* set 1, where %NSA declined from 50% to 17% at 64 °C and from 50% to 0% at 68 °C, with TTN values correspondingly extended. The M13 bacteriophage set, previously NSA-resistant, also showed modest but consistent gains in TTN with ssBP, indicating a stabilizing effect even in high-fidelity systems.

Under the most stringent conditions tested—68 °C in the presence of 22.8 μM ssBP—seven of the eight primer sets were completely free of significant detectable NSA (Table 2). The sole exception was *E. coli* set 1, which produced a late-rising NTC signal (Fig. 3). Melt analysis and 16S qPCR attributed this fluorescence to trace *E. coli* genomic DNA carried over with the recombinant ssBP, corresponding to roughly 20–60 contaminating copies per reaction (data not shown). Because ssBP can also bind double-stranded DNA in addition to single-stranded DNA, albeit with lower affinity, this background precludes any fair assessment of ssBP's effect on *E. coli*-targeted assays. By contrast, the *M. tuberculosis* (*rpoB*) traces never exceeded 10% of the fluorescence of their positive controls and appeared only at the end of the assay; we therefore classified them as negative (Table 2; Fig. 3; Supplementary Fig. S2). The results obtained confirm that pairing high-stringency temperature with thermolabile ssBP is an efficient strategy to suppress NSA for every target tested except where reagent-borne DNA contamination is present. This supports a mechanistic model in which LAMP specificity depends not only on primer design or reaction temperature, but also on early primer accessibility during the pre-amplification phase.

Resolving residual NSA with ssBP at high temperatures

To determine whether the combined application of elevated temperature and thermolabile single-stranded DNA-binding protein (ssBP) can fully suppress residual nonspecific amplification (NSA), we revisited a subset of primer sets previously shown to exhibit persistent NSA at 69 °C (Table 1). These included six targets used for the detection of *C. auris*, *S. agalatiae*, *M. tuberculosis*, and hepatitis B virus DNA, which remained vulnerable to misamplification despite high-temperature assay conditions. *E. coli* targets were excluded owing to the inherent contamination of ssBP with template DNA. Each primer set was reassessed at 69 °C in the absence or presence of 22.8 μM ssBP, and performance was evaluated in terms of time to result (TTR), time to NTC (TTN), and percentage of NSA (%NSA). The results are summarized in Table 3.

Remarkably, the incorporation of ssBP led to complete suppression of NSA in five out of six cases. The lone exception was the *C. auris* primer set, where %NSA, though not entirely eliminated, was significantly reduced from 100%, in the absence of ssBP, to 33% with ssBP. Notably, amplification kinetics (TTR) were preserved in all reactions, consistent with prior observations at 64–68 °C. These findings confirm that the combined strategy of operating at 69 °C and including ssBP effectively all but eliminates even the most persistent cases of NSA.

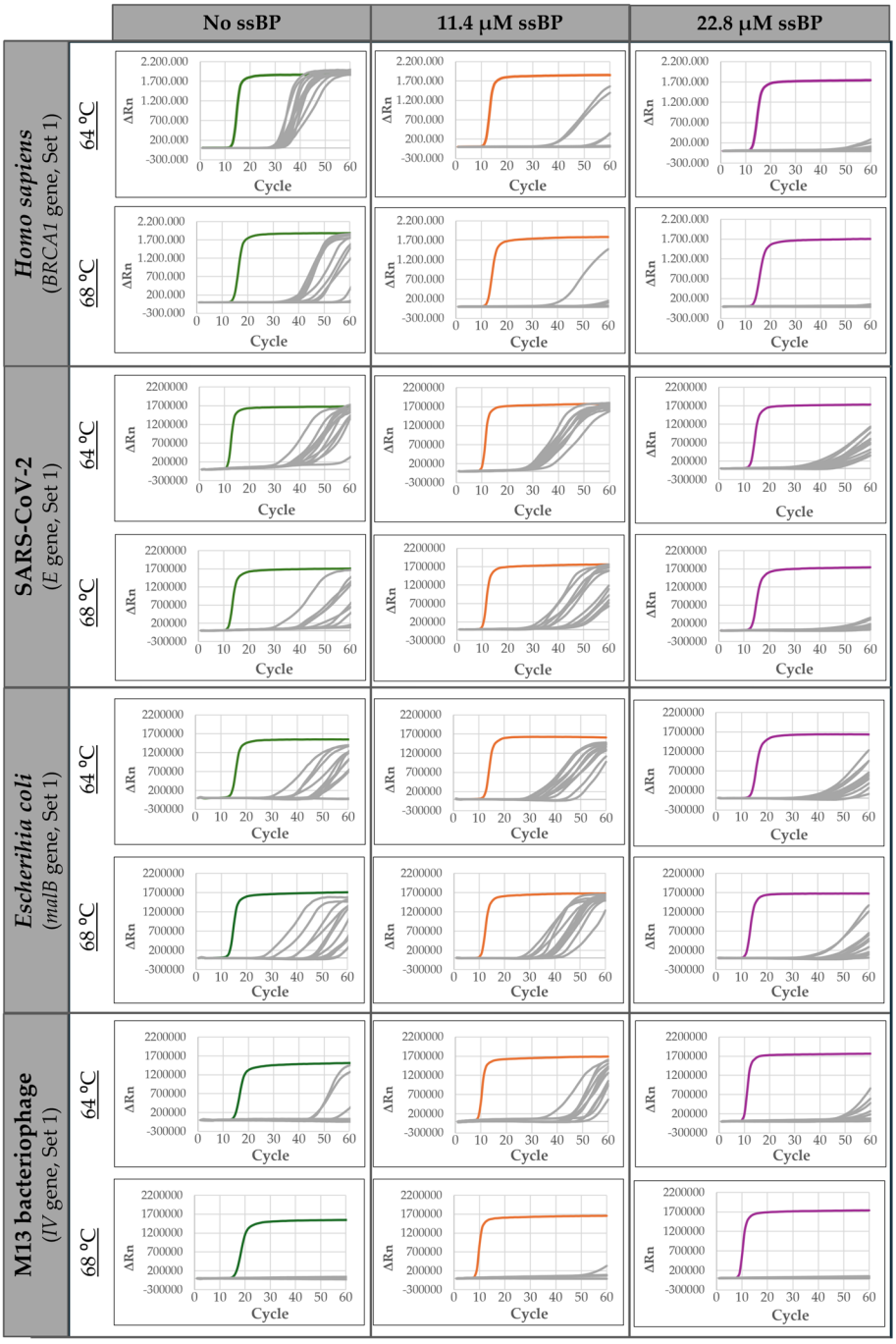


Fig. 3 Effect of reaction temperature and ssBP on nonspecific amplification in LAMP assays. Representative real-time amplification curves illustrate the influence of increased reaction temperature (64 and 68 °C) and single-stranded DNA-binding protein (ssBP) concentration (0, 11.4, and 22.8 µM) on amplification profiles using eight selected LAMP primer sets, here exemplified for *BRCA1*, *E* gene, *malB*, and gene *IV*. All reactions were performed with 10^5 copies of target DNA (positive controls) or without template (NTCs). Amplification traces for NTCs are shown in grey to highlight the impact of ssBP on nonspecific amplification (NSA). Each cycle represents 30 s, totaling 30 min for the full assay duration. Full quantitative metrics, including TTR, TTN, and %NSA, are summarized in Table 2

Table 3 Impact of single-stranded DNA-binding protein (ssBP) on LAMP amplification kinetics and specificity at 69 °C

		TTR (min)		TTN (min)		NSA (%)	
[ssBP]		**0 µM**	**22.8 µM**	**0 µM**	**22.8 µM**	**0 µM**	**22.8 µM**
***C. auris* (*PFO* gene)**	**Set 2**	**5.69**	**4.33**	**19.40**	**23.29**	**100**	**33.3**
S. agalatiae (*FbsB* gene)	Set 1	5.88	6.09	27.04	–	56.6	0.00
M. tuberculosis (*rpoB* gene)	Set 1	10.07	12.76	25.86	–	22.2	0.00
Hepatitis B virus (*P* gene)	Set 1	5.03	5.01	15.33	–	100	0.00
	Set 2	4.51	4.53	19.29	–	100	0.00
	Set 3	8.60	7.40	25.22	–	56.6	0.00
Average		6.63	6.69	22.02	–	72.2	–

Six challenging LAMP primer sets were tested at 69 °C in the presence of 0 or 22.8 µM ssBP. Amplification performance was evaluated by time to result (TTR, min), time-to-no-template control signal (TTN, min), and percentage of nonspecific amplification (%NSA). The TTR values reflect amplification speed in the presence of target DNA. TTN values indicate the time at which amplification was detected in no-template controls, and %NSA represents the proportion of NTC replicates showing amplification within 30 min. Missing TTN values ("–") indicate no detectable signal during the assay time frame. Average values across all sets are shown in the last row

Performance of liquid and lyophilized LAMP master mixes for real-time and colorimetric detection

Expanding on the mechanistic findings of the previous sections, particularly the influence of elevated temperature and early primer mispriming on NSA, we next assessed whether these findings could be translated into improved diagnostic performance by using LAMP master mixes under simulated laboratory and point-of-care conditions. Nine of the previously validated primer sets, showing robust amplification—*H. sapiens*, *C. auris*, *C. albicans*, *E. coli*, *L. interrogans*, *M. tuberculosis*, two SARS-CoV-2 loci, and M13 phage—were selected as representative targets. Two distinct master mix formulations were developed: (i) a real-time fluorescence-based master mix optimized for laboratory use and (ii) a colorimetric master mix intended for point-of-care applications. Both mixes were engineered to be lyophilization-ready, allowing direct comparison of fresh and freeze-dried formats. To rigorously test their performance, each formulation was challenged with serial dilutions of starting DNA (10^7 to 10 copies) and no-template controls (NTCs), under standardized amplification conditions at 69 °C. Liquid and reconstituted lyophilized mixes were assayed side-by-side to evaluate any loss of activity after freeze-drying. The results are exemplified in Fig. 4 and combined in Supplementary Fig. S3.

The real-time master mix performed robustly across all targets, with amplification being detected with input levels as low as 10 copies for SARS-CoV-2 *N2* and *E. coli*, 100 copies for *C. albicans* and SARS-CoV-2 *E*, and 1000 copies for the remaining targets. These observed differences in LAMP sensitivity across targets have previously been attributed to multiple primer- and template-specific factors [36]. In general, the lyophilized master mix format closely matched the sensitivity of the liquid counterpart, demonstrating that the freeze-drying step did not compromise enzymatic activity or overall assay integrity. A slight reduction in sensitivity was observed for the lyophilized format in *E. coli,* where the detection limit increased from 10 to 100 copies (Fig. 4). In addition, the real-time amplification curves displayed high reproducibility and low variability across template concentrations, suggesting that the formulation is both precise, sensitive and specific. Finally, incorporation of previous insights concerning reaction accuracy

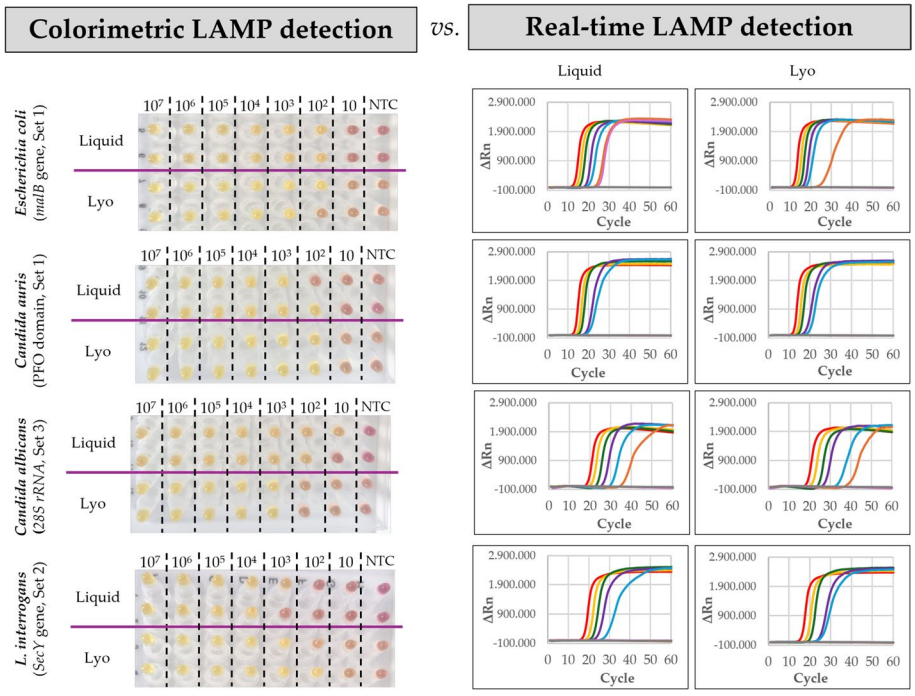


Fig. 4 Comparative performance of colorimetric and real-time LAMP in liquid and lyophilized formats. Representative data from four selected targets—*E. coli* (*malB* gene), *C. auris* (*PFO* domain), *C. albicans* (25S rRNA gene) and *L. interrogans* (*SecY* gene)—demonstrate the sensitivity and robustness of the developed master mixes. Reactions were conducted at 69 °C using serial dilutions of template DNA, ranging from 10^7 to 10 copies per reaction. Each master mix was tested in both liquid and lyophilized (reconstituted) forms. For colorimetric assays (left panels), successful amplification is indicated by a yellow color shift, while pink denotes no amplification. For real-time fluorescence detection (right panels), amplification curves are shown in distinct colors representing template concentrations: 10^7 (red), 10^6 (yellow), 10^5 (green), 10^4 (purple), 10^3 (blue), 10^2 (orange), and 10 (pink) copies. The data illustrates comparable performance across formats and methods, confirming the preservation of sensitivity and specificity following lyophilization and supporting the utility of both formulations for point-of-care and laboratory-based diagnostics. Each cycle represents 30 s, totaling 30 min for the full assay duration

ensured that all reactions remained highly specific, with no amplification observed in NTCs.

Colorimetric LAMP reactions, using pH-sensitive dye-based detection, also demonstrated excellent performance (Fig. 4; Supplementary Fig. S3). A clear pink-to-yellow shift distinguished positive and negative reactions with high contrast. While colorimetric sensitivity was slightly lower than real-time fluorescence-based detection, typically detecting down to 100 or 1000 copies, it remained within acceptable diagnostic thresholds for high-prevalence pathogens. This contrast between colorimetric and real-time LAMP detection limits has been reported before in literature [37], however the difference we observed was not as pronounced. In addition, both liquid and lyophilized colorimetric mixes yielded similar results, with minimal variation in visual output, confirming the robustness of the lyophilized formulation. Fluorescence-based assays provide real-time monitoring and higher resolution, while pH-dependent colorimetric systems require bulk acidification, which may delay visible changes at very low template concentrations [30, 38, 39].

The consistency between fluorescent and colorimetric configurations, in both liquid and lyophilized formats, further supports the idea that NSA in LAMP is primarily dictated by primer–primer interactions during the pre-amplification phase and is not significantly influenced by the physical format of the reaction mix. Given that all reactions

were conducted at 69 °C, a temperature previously shown to mitigate NSA when combined with optimized primer design and single-stranded DNA-binding proteins, the absence of amplification in NTCs reinforces the notion that specificity can be maintained through rational reaction design.

Resistance of lyo-compatible LAMP mixes to common diagnostic inhibitors

Given the growing demand for molecular diagnostic tools compatible with minimally processed or crude samples, it is imperative to ensure assay robustness in the presence of common inhibitory substances. Following the systematic optimization strategies described in the preceding sections, we next evaluated the tolerance of the different LAMP formulations to a panel of clinically and environmentally relevant inhibitors. Specifically, we assessed both real-time and colorimetric liquid LAMP master mixes using a SARS-CoV-2 *E* gene target (10^5 DNA copies/reaction) in the presence of increasing concentrations of seven representative inhibitors (Supplementary Table S4). The selected inhibitors included: (i) biological contaminants, exemplified by hemoglobin, plasma, serum, saliva, bile salts and urine, and (ii) extraction reagent residues, represented by the common sample contaminant ethanol. These agents are widely recognized for their ability to impair nucleic acid amplification by interfering with polymerase activity, chelating magnesium ions, or disrupting nucleic acid hybridization [40]. Although qPCR is notoriously susceptible to such inhibitors, LAMP is generally considered more tolerant to these compounds [16, 40].

The data (Fig. 5) revealed that colorimetric assays appear to display higher vulnerability to inhibitors when compared with real-time LAMP results, with several substances inducing ambiguous or misleading color changes even at moderate concentrations (Fig. 5, left). We postulate that this could be due to the inherent pigmentation of these inhibitors (e.g., hemoglobin) or their buffering capacity (e.g., bile salts), which ultimately interferes with pH-based detection. Nonetheless, colorimetric LAMP inhibition is still very poorly characterized in the literature, limiting result interpretation. Recent studies have reported that combining dyes in different ratios can lead to a more robust colorimetric detection [41, 42], therefore this could be an avenue worth exploring in future work by combining Cresol Red with, for example, a pH-insensitive dye. Notably, pH-independent colorimetric LAMP methods have been developed [43] by using a divalent zinc salt (such as $ZnCl_2$) and murexide to form a transient complex (Zn-MX). However, since zinc can only be added after the reaction because it inhibits DNA amplification, this increases the risk of carryover contamination and, subsequently, false positive results, rendering it unsuitable for routine use in diagnostics.

Conversely, real-time assays using fluorescent detection demonstrated considerable resilience (Fig. 5, right) to the tested inhibitors. Real-time amplification remained effective across a broad range of inhibitor concentrations, maintaining clear amplification curves and time-to-result metrics with minimal delay, at least for the two first inhibitor concentrations tested. The only compounds that posed a bigger challenge were bile salts and ethanol, which were previously demonstrated to have a greater inhibitory effect in DNA amplification reactions [16, 40, 44]. Regardless, resistance to inhibitors had a consistent pattern across both real-time and colorimetric formats, suggesting that the core LAMP formulation itself—optimized in the current study through thermostable components and the minimization of NSA—is inherently resilient. However, signal detection

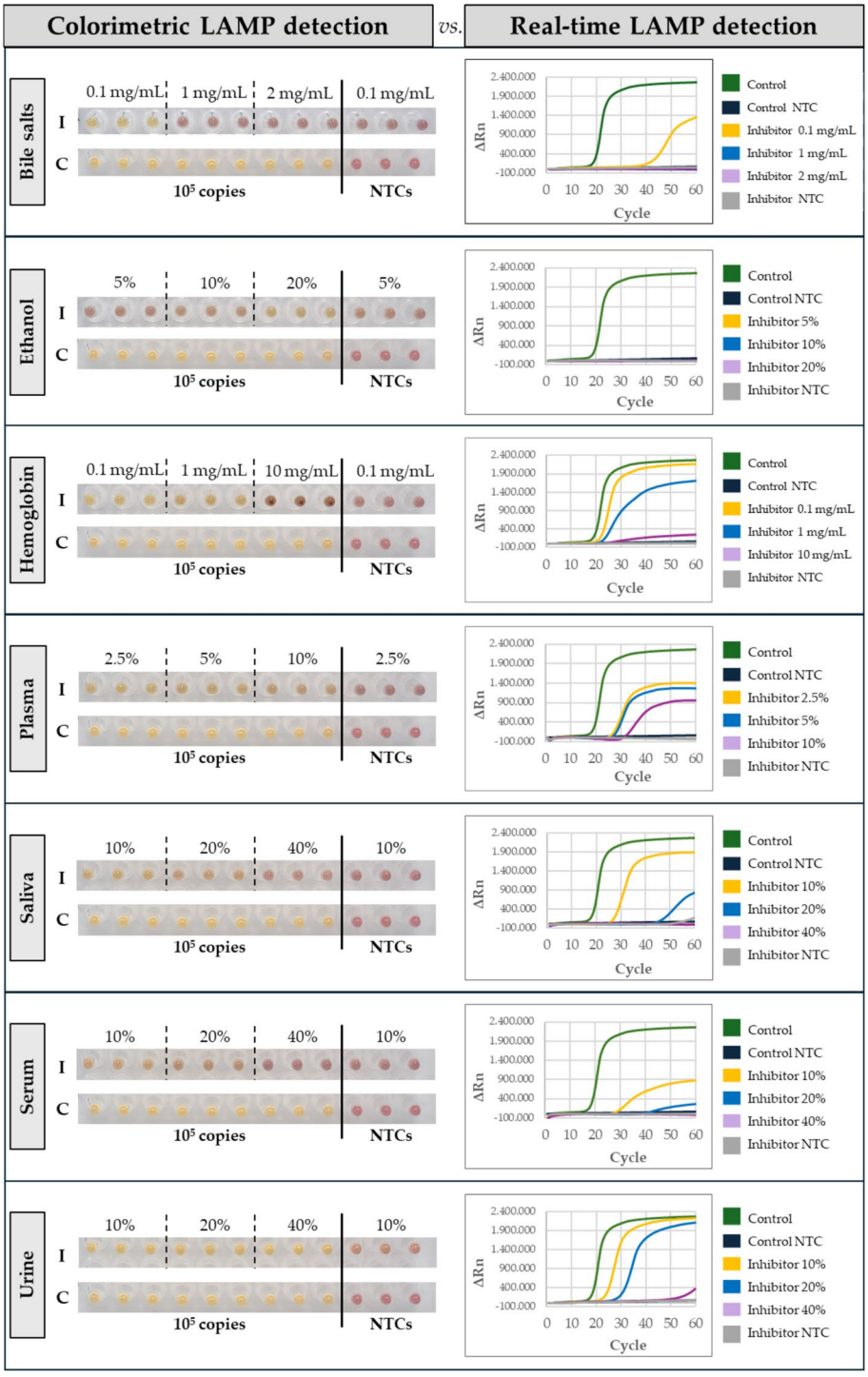


Fig. 5 Resistance of optimized real-time and colorimetric LAMP master mixes to common diagnostic inhibitors. LAMP assays targeting the SARS-CoV-2 *E* gene (10^5 DNA copies/reaction) were performed using either the real-time fluorescence-based (right) or the pH-sensitive colorimetric (left) master mixes in liquid format. Each reaction was challenged with increasing concentrations of seven representative inhibitors, including common biological contaminants and ethanol. Fluorescence amplification curves (right) and endpoint color changes (left) are shown for each condition. Each cycle represents 30 s, totaling 30 min for the full assay duration. All reactions were performed in technical triplicates

modality significantly modulates practical diagnostic reliability in contaminated contexts [37]. These results confirm the superior robustness of fluorescence-based real-time LAMP for inhibitor-rich matrices and underscore the limitations of pH-dependent colorimetric detection when applied to complex clinical samples.

Analytical validation of high-temperature ssBP-LAMP comparatively to qPCR

Although high-temperature ssBP-LAMP emerged in this study as a robust strategy for pathogen detection, quantitative PCR (qPCR) remains the gold standard for nucleic acid detection in molecular diagnostics [45]. We therefore benchmarked ssBP-LAMP directly against standard qPCR assays using biologically relevant sample matrices. *Escherichia coli* cells were used to spike human urine, alongside water controls, and the *malB* gene was detected using three real-time methods: TaqMan qPCR, SYBR Green qPCR, and ssBP-LAMP. To avoid locus-dependent bias, the F3 and B3 primers of the ssBP-LAMP target were also used as the amplification primers in the two qPCR formats. The use of crude and extracted samples allowed the testing of inhibitor resistance and lysis efficiency under conditions relevant to diagnostic workflows.

The results, presented in Table 4 and Fig. 6, revealed that high-temperature ssBP-LAMP displayed a similar detection performance when compared with qPCR across the full range of tested bacterial loads (200 to 2×10^5 copies per reaction), which represent concentrations commonly reported in urine samples infected with *E. coli* [46]. Across all concentrations, ssBP-LAMP consistently detected the target in both water and urine matrices, demonstrating matrix-independent robustness and supporting the inhibitor tolerance observed in earlier sections. When compared with SYBR qPCR, which relies on the same intercalating dye-based fluorescence chemistry, ssBP-LAMP showed superior robustness in urine, particularly in nonextracted samples, as illustrated in the left panels of Fig. 6. This highlights the resilience of the ssBP-LAMP chemistry to urine-associated inhibitors that negatively impact conventional qPCR amplification.

Analysis of extracted versus crude samples revealed a larger time-to-threshold shift for ssBP-LAMP than for qPCR, reflected by higher ΔC_t values (Table 4). This effect is expected and can be attributed to fundamental mechanistic differences between the techniques. Because LAMP is isothermal and operates at a lower temperature than qPCR, cell lysis is less efficient and reduced template accessibility is expected in crude samples, whereas nucleic acid extraction markedly accelerates target availability [45]. Importantly, despite this kinetic delay, ssBP-LAMP retained reliable detection across all tested conditions. Together, these findings establish that high-temperature ssBP-LAMP provides analytical performance comparable to qPCR while enabling direct testing of nonextracted samples. This combination directly addresses key cost and time constraints associated with conventional qPCR-based diagnostics.

Discussion

Loop-mediated isothermal amplification (LAMP) is a nucleic acid amplification method that has gained prominence for its speed and operational simplicity [5, 7, 47]. Despite increasing interest and its potential to replace qPCR in decentralized settings, the broader adoption of LAMP in molecular diagnostics has been generally limited by its susceptibility to nonspecific amplification (NSA), particularly under suboptimal primer configurations or reaction conditions [8–10]. This study provides a systematic evaluation

Table 4 Comparison of C_t values obtained for the detection of *Escherichia coli* (*malB*) by three distinct techniques: TaqMan qPCR (qPCR Probe), SYBR Green PCR (qPCR SYBR), and ssBP-LAMP (ssBP-LAMP), in direct and extracted spiked urine and control samples

		C_t mean*					
Sample		**Urine**			**Control**		
Extraction		**No**	**Yes**	**Δ C_t**	**No**	**Yes**	**Δ C_t**
2×10^5 copies	qPCR Probe	20.54	20.91	− 0.37	21.97	21.64	0.33
	qPCR SYBR	20.07	18.27	1.80	19.17	17.84	1.32
	ssBP-qLAMP	16.98	11.85	5.12	14.98	12.35	2.64
2×10^4 copies	qPCR Probe	23.59	24.80	− 1.22	25.24	26.04	−0.80
	qPCR SYBR	22.64	22.96	− 0.32	22.17	21.81	0.37
	ssBP-qLAMP	19.25	14.62	4.63	17.08	14.67	2.42
10,000 copies	qPCR Probe	25.33	25.93	− 0.60	26.27	26.79	−0.52
	qPCR SYBR	24.19	23.94	0.26	23.07	22.42	0.65
	ssBP-qLAMP	20.23	15.23	5.00	18.51	14.89	3.62
5000 copies	qPCR Probe	25.86	27.07	− 1.20	27.13	28.03	−0.89
	qPCR SYBR	24.83	25.73	− 0.90	24.18	23.80	0.38
	ssBP-qLAMP	21.00	15.96	5.04	18.76	15.89	2.87
2000 copies	qPCR Probe	27.11	28.44	− 1.34	28.12	29.82	−1.70
	qPCR SYBR	25.94	27.44	− 1.50	25.76	25.11	0.65
	ssBP-qLAMP	22.49	16.70	5.78	19.62	16.87	2.75
1000 copies	qPCR Probe	28.40	29.51	− 1.11	29.01	30.17	−1.16
	qPCR SYBR	27.50	27.94	− 0.44	26.37	26.15	0.22
	ssBP-qLAMP	24.96	16.95	8.01	20.45	17.16	3.29
200 copies	qPCR Probe	30.26	31.59	− 1.33	30.67	33.11	−2.44
	qPCR SYBR	29.90	30.79	− 0.89	28.99	28.25	0.74
	ssBP-qLAMP	28.49	19.36	914	21.40	18.76	2.64

Three real-time amplification methods were employed to detect *E. coli* in both direct (nonextracted) and extracted spiked urine and water control samples, allowing for a comparative assessment of analytical sensitivity and matrix effects. The samples tested contained an initial number of cells, allowing for a final concentration of genomic DNA ranging between 200 and 2×10^5 copies/reaction. Δ C_t was calculated as the difference between the cycle threshold value obtained for nonextracted samples with no extraction and their extracted counterparts

* For ssBP-LAMP, the reported C_t values correspond to time-to-threshold (TTR) measurements rather than amplification cycles, as ssBP-LAMP is an isothermal reaction and does not involve thermal cycling. In the real-time acquisition used here, fluorescence was recorded every 30 s; therefore, ssBP-LAMP C_t values can be converted to time in minutes by dividing by 2

of the determinants of LAMP specificity and robustness and delivers a unifying strategy to overcome its most persistent limitations, thereby enabling a more predictable and broadly deployable diagnostic platform.

LAMP primer design is inherently complex. A standard reaction may require up to six primers at varying concentrations, and unlike qPCR, fewer than a dozen publicly available tools exist to support LAMP primer design [48]. To uncover the origins of NSA, we tested 21 primer sets targeting diverse genomic sequences from a wide range of organisms. Our results identify the core primer sets (FIP/BIP and F3/B3) as primary drivers of specificity, with loop primers playing a more modest role. Importantly, thermodynamic parameters alone proved insufficient to predict NSA, highlighting the lack of computational tools adapted to the isothermal context. Local template structures, primer accessibility, and stochastic interactions likely contribute to amplification artifacts and remain largely unexplored in LAMP workflows.

We previously showed that thermostable strand-displacing polymerases enable high-temperature LAMP (≥ 68 °C), potentially reducing the prevalence of NSA [16]. However, the present study shows that increasing the reaction temperature by using a thermostable strand displacement polymerase is insufficient to fully eliminate nonspecific

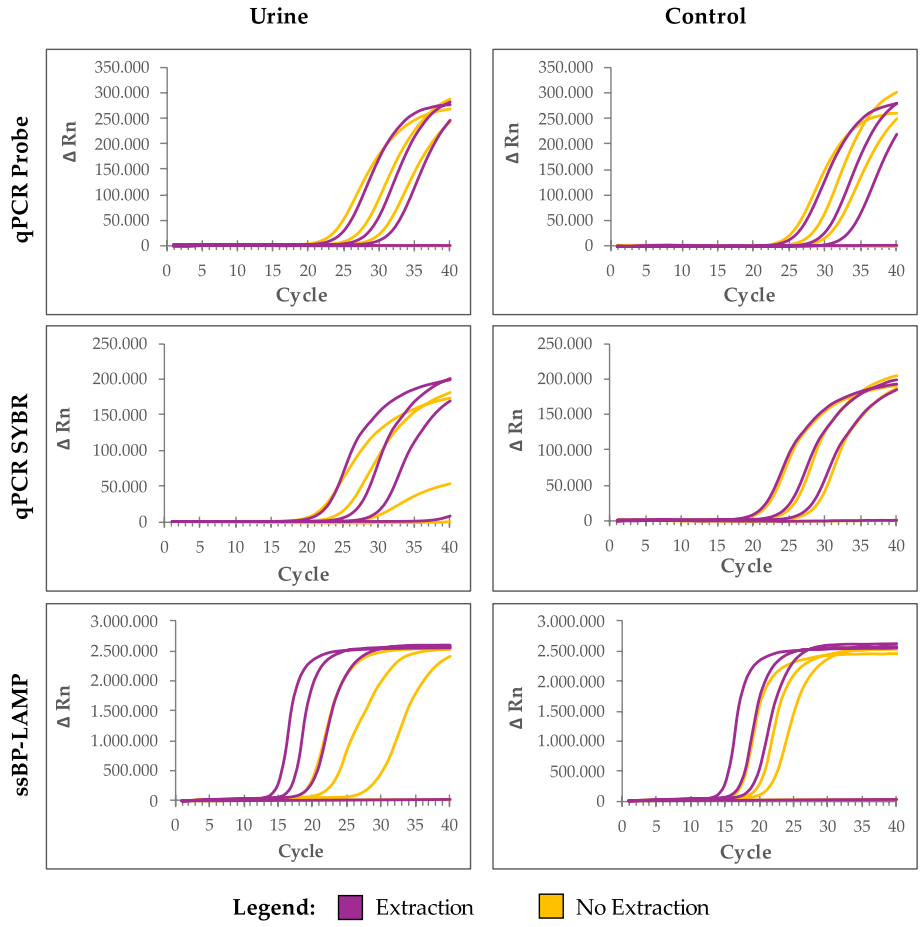


Fig. 6 Detection of *E. coli* (*malB*) by three distinct techniques: real-time Probe PCR (qPCR Probe), TaqMan qPCR (qPCR Probe), SYBR Green PCR (qPCR SYBR), and ssBP-LAMP (ssBP-LAMP), in direct and extracted spiked urine and control samples. Real-time assays targeting the *E. coli malB* gene were performed using spiked urine and control samples that were either analyzed directly (nonextracted) (yellow) or subjected to nucleic acid extraction (purple). The initial genomic DNA concentrations used per reaction were serial dilutions estimated to be 20,000, 2000, and 200 copies and appear in this respective succession from left to right in all charts. All reactions were performed in technical triplicates

amplification, as early primer–primer interactions during the thermal ramp-up phase remain a hidden but decisive source of false positives. To address this early-phase vulnerability, we introduced a thermolabile single-stranded DNA-binding protein (ssBP) from *Escherichia* phage T7, which transiently sequesters primers and mitigates nonspecific hybridization [34]. When combined with conventional LAMP primers and elevated assay temperatures (≥ 68 °C), a concentration of 22.8 µM of ssBP yielded highly specific diagnostic assays and efficiently eliminated nonspecific amplification even for the most challenging targets screened. Together, the data suggest that this dual-parameter optimization, including ssBP and high-temperature LAMP, offers a robust pathway to enhance assay specificity without compromising amplification performance and is readily applicable to molecular diagnostics where high specificity is essential.

Although LAMP has the advantage of being a simpler and faster technique, there are often concerns regarding its sensitivity as qPCR has been proven to have lower limits of detection (LoD) [49, 50]. Detection thresholds vary by target and detection modality [9, 30], and LAMP's performance has historically been difficult to generalize. By integrating

the ssBP strategy into both real-time fluorescence and colorimetric master mixes, we established formats that are compatible with lyophilization and field use. The real-time assays consistently achieved detection limits of 10–100 copies across nine diagnostically and environmentally relevant targets, while the colorimetric format retained visual sensitivity in the 100–1000 copy range, which is optimal for point-of-care deployment. Moreover, results obtained with crude and extracted spiked samples demonstrate that ssBP-LAMP achieves analytical performance comparable to qPCR for this matrix, while providing faster detection and increased robustness in urine-containing samples. Indeed, multiple studies have shown that LAMP is generally more tolerant to clinical, environmental, and nucleic acid extraction inhibitors when compared with qPCR [40, 51]. Our results confirmed the resistance of ssBP-LAMP to a panel of common clinical inhibitors, including plasma, hemoglobin, saliva, and urine, and indicate that the real-time master mix exhibits a higher tolerance than the colorimetric format. These differences in resistance could be due to the inherent pigmentation of some inhibitors (e.g., hemoglobin) or their buffering capacity (e.g., bile salts) that directly interfere with the pH-based color detection mechanism. Together, these findings underscore the versatility of high-temperature LAMP (≥ 68 °C) when supplemented with a thermolabile ssBP and offer a generalizable strategy with broad applicability across a diversity of diagnostic scenarios.

Conclusions

This work transitions LAMP from a method constrained by static thermodynamic and design limitations to a dynamic and tunable high-performance amplification platform. By synchronizing temperature control with primer availability through the use of ssBP, we offer a robust, generalizable solution to nonspecific amplification. In addition to qPCR-comparable sensitivity and efficiency, ssBP-LAMP exhibits a high degree of tolerance to clinically relevant inhibitors, including plasma, hemoglobin, saliva, and urine. Comparative benchmarking against established qPCR assays further confirms that ssBP-LAMP operates at a level consistent with current gold-standard molecular diagnostic workflows. This advance is a major step in the evolution of isothermal diagnostics and restores the full diagnostic potential of LAMP by promoting its deployment in settings ranging from centralized laboratories to point-of-care environments.

Abbreviations

IMAC	Immobilized metal ion affinity chromatography
LIC	Ligation independent cloning
LAMP	Loop-mediated isothermal amplification
Tm	Melting temperature
NTC	No-template control
NSA	Nonspecific amplification
POC	Point-of-care
PCR	Polymerase chain reaction
qPCR	Quantitative PCR
ssBP	Single-stranded DNA-binding protein
TTN	Time to NTC
TTR	Time to result

Supplementary Information

The online version contains supplementary material available at https://doi.org/10.1186/s11658-026-00926-8.

Additional file 1.

Additional file 2.

Additional file 3.

Acknowledgements
Not applicable.

Author contributions
Conceptualization, R.S. and C.F.; methodology, R.S. and J.T.; software, R.S. and J.T; formal analysis, R.S., C.F. and J.T.; writing—original draft preparation, R.S.; writing—review and editing, J.T., C.F. and P.B.; supervision, C.F., J.T. and P.B.; funding acquisition, C.F. All authors have read and agreed to the published version of the manuscript.

Funding
This research was funded by a Portugal2030 project (Lisbon, Portugal; DiagnosTech, grant no. 14422).

Availability of data and materials
The datasets used and/or analyzed during the current study are available in the following online repository: https://tinyurl.com/uecyukd6.

Declarations

Ethics approval and consent to participate
Not applicable.

Consent for publication
Not applicable.

Competing interests
R.S., J.T., and C.F. are employed by NZYtech, Lda., a biotechnology company dedicated to the production of enzymes. All other authors declare they have no competing interests.

Received: 1 September 2025 / Accepted: 30 March 2026
Published online: 16 April 2026

References

1. Mullis K, Faloona F, Scharf S, Saiki R, Horn G, Erlich H. Specific enzymatic amplification of DNA in vitro: the polymerase chain reaction. Cold Spring Harb Symp Quant Biol. 1986;51:263–73.
2. Mullis KB, Faloona FA. Specific synthesis of DNA in vitro via a polymerase-catalyzed chain reaction. Methods Enzymol. 1987;(155):335–50.
3. Esbin MN, Whitney ON, Chong S, Maurer A, Darzacq X, Tjian R. Overcoming the bottleneck to widespread testing: a rapid review of nucleic acid testing approaches for COVID-19 detection. RNA. 2020;26(7):771–83.
4. Shen M, Zhou Y, Ye J, Abdullah AL-maskri AA, Kang Y, Zeng S, et al. Recent advances and perspectives of nucleic acid detection for coronavirus. J Pharm Anal. 2020;10(2):97–101.
5. Notomi T. Loop-mediated isothermal amplification of DNA. Nucleic Acids Res. 2000;28(12):63e–63.
6. Notomi T, Mori Y, Tomita N, Kanda H. Loop-mediated isothermal amplification (LAMP): principle, features, and future prospects. J Microbiol. 2015;53(1):1–5.
7. Nagamine K, Hase T, Notomi T. Accelerated reaction by loop-mediated isothermal amplification using loop primers. Mol Cell Probes. 2002;16(3):223–9.
8. Srivastava P, Prasad D. Isothermal nucleic acid amplification and its uses in modern diagnostic technologies. 3 Biotech. 2023;13(6):200.
9. Wang DG, Brewster J, Paul M, Tomasula P. Two methods for increased specificity and sensitivity in loop-mediated isothermal amplification. Molecules. 2015;20(4):6048–59.
10. Shirshikov FV, Bespyatykh JA. Loop-mediated isothermal amplification: from theory to practice. Russ J Bioorganic Chem. 2022;48(6):1159–74.
11. Padzil F, Mariatulqabtiah AR, Tan WS, Ho KL, Isa NM, Lau HY, et al. Loop-mediated isothermal amplification (LAMP) as a promising point-of-care diagnostic strategy in avian virus research. Animals. 2021;12(1):76.
12. Ye J, Coulouris G, Zaretskaya I, Cutcutache I, Rozen S, Madden TL. Primer-BLAST: a tool to design target-specific primers for polymerase chain reaction. BMC Bioinformatics. 2012;13(1):134.
13. Mohamed Sedek SA, Arifin MA, Abdul Munaim MS. qPCR analysis of quorum sensing genes of *Pseudomonas aeruginosa*: primer design and qPCR efficiency. Int J Eng Technol Sci. 2023;10(1):43–50.
14. Jang M, Kim S. Inhibition of non-specific amplification in loop-mediated isothermal amplification via tetramethylammonium chloride. BioChip J. 2022;16(3):326–33.
15. Zhang Y, Ren G, Buss J, Barry AJ, Patton GC, Tanner NA. Enhancing colorimetric loop-mediated isothermal amplification speed and sensitivity with guanidine chloride. Biotechniques. 2020;69(3):178–85.
16. Simões RSRM, Teodoro JPST, Gomes PMB, De Andrade Fontes CMG. Bringing the heat: thermostable analogs of Bst polymerase allow high-temperature LAMP. Eur J Clin Invest. 2025;13:e70071.
17. Shang Y, Sun J, Ye Y, Zhang J, Zhang Y, Sun X. Loop-mediated isothermal amplification-based microfluidic chip for pathogen detection. Crit Rev Food Sci Nutr. 2020;60(2):201–24.
18. Tanner NA, Evans TC. Loop-mediated isothermal amplification for detection of nucleic acids. Curr Protoc Mol Biol [Internet]. 2014 Jan [cited 2025 Jun 30];105(1). Available from: https://doi.org/10.1002/0471142727.mb1514s105
19. Yamamoto M, Alshahni MM, Tamura T, Satoh K, Iguchi S, Kikuchi K, et al. Rapid detection of candida Auris based on loop-mediated isothermal amplification (LAMP). J Clin Microbiol. 2018;56(9):e00591–18.

20. Wang Y, Zhao X, Zhou Y, Lu J, Yu H, Li S. Establishment and application of loop-mediated isothermal amplification coupled with nanoparticle-based lateral flow biosensor (LAMP-LFB) for visual and rapid diagnosis of Candida albicans in clinical samples. Front Bioeng Biotechnol. 2022;7(10):1025083.
21. Othman S, Lee PY, Lam JY, Philip N, Azhari NN, Affendy NB, et al. A versatile isothermal amplification assay for the detection of leptospires from various sample types. PeerJ. 2022;10(10):e12850.
22. Chen HW, Belinskaya T, Zhang Z, Ching WM. Simple detection of hepatitis B virus in using loop-mediated isothermal amplification method. Mil Med. 2019;184(7–8):e275–80.
23. Ching WM, Chao CC, Chen HW. Detection of hepatitis B virus in blood using LAMP method. WO 2012/108961 A1. 2012.
24. Kim YT, Tabor S, Bortner C, Griffith JD, Richardson CC. Purification and characterization of the bacteriophage T7 gene 2.5 protein. A single-stranded DNA-binding protein. J Biol Chem. 1992;267(21):15022–31.
25. Tiwari P, Kaila P, Guptasarma P. Understanding anomalous mobility of proteins on SDS-PAGE with special reference to the highly acidic extracellular domains of human E- and N-cadherins. Electrophoresis. 2019;40(9):1273–81.
26. Zhang Y, Odiwuor N, Xiong J, Sun L, Nyaruaba RO, Wei H, et al. Rapid molecular detection of SARS-CoV-2 (COVID-19) virus RNA using colorimetric LAMP [Internet]. 2020 [cited 2025 Jun 20]. Available from: https://doi.org/10.1101/2020.02.26.20028373
27. Mori Y, Notomi T. Loop-mediated isothermal amplification (LAMP): a rapid, accurate, and cost-effective diagnostic method for infectious diseases. J Infect Chemother. 2009;15(2):62–9.
28. Tomita N, Mori Y, Kanda H, Notomi T. Loop-mediated isothermal amplification (LAMP) of gene sequences and simple visual detection of products. Nat Protoc. 2008;3(5):877–82.
29. Oscorbin IP, Shevelev GYu, Pronyaeva KA, Stepanov AA, Shamovskaya DV, Mishukova OV, et al. Detection of SARS-CoV-2 RNA by a multiplex reverse-transcription loop-mediated isothermal amplification coupled with melting curves analysis. Int J Mol Sci. 2021;22(11):5743.
30. Tanner NA, Zhang Y, Evans TC. Visual detection of isothermal nucleic acid amplification using pH-sensitive dyes. Biotechniques. 2015;58(2):59–68.
31. Oscorbin I, Filipenko M. Bst polymerase—a humble relative of Taq polymerase. Comput Struct Biotechnol J. 2023;21:4519–35.
32. Dickey TH, Altschuler SE, Wuttke DS. Single-stranded DNA-binding proteins: multiple domains for multiple functions. Structure. 2013;21(7):1074–84.
33. Ashton NW, Bolderson E, Cubeddu L, O'Byrne KJ, Richard DJ. Human single-stranded DNA binding proteins are essential for maintaining genomic stability. BMC Mol Biol. 2013;14(1):9.
34. Kur J, Olszewski M, Długołecka A, Filipkowski P. Single-stranded DNA-binding proteins (SSBs)—sources and applications in molecular biology. Acta Biochim Pol. 2005;52(3):569–74.
35. Hollis T, Stattel JM, Walther DS, Richardson CC, Ellenberger T. Structure of the gene 2.5 protein, a single-stranded DNA binding protein encoded by bacteriophage T7. Proc Natl Acad Sci. 2001;98(17):9557–62.
36. Wang C, Xu Z, Hou X, Wang M, Zhou C, Liang J, et al. Rapid, sensitive, specific, and visual detection of Salmonella in retail meat with loop-mediated isothermal amplification, targeting the invA gene. J Food Prot. 2022;85(1):6–12.
37. Atceken N, Asghari Dilmani S, Abdullah AC, Sarıkaya M, Yigci D, Korkmaz G, et al. Development and validation of LAMP assays for distinguishing MPXV clades with fluorescent and colorimetric readouts. Biosensors. 2025;15(1):23.
38. Novi VT, Meher AK, Abbas A. Visualization methods for loop mediated isothermal amplification (LAMP) assays. Analyst. 2025;150(4):588–99.
39. Arunrut N, Kampeera J, Dangtip S, Pengpanich S, Khumwan P, Kiatpathomchai W. Development of colorimetric triplex reverse transcription loop-mediated isothermal amplification for rapid and sensitive detection of shrimp yellow head virus (YHV). Aquac Int. 2025;33(2):91.
40. Nwe MK, Jangpromma N, Taemaitree L. Evaluation of molecular inhibitors of loop-mediated isothermal amplification (LAMP). Sci Rep. 2024;14(1):5916.
41. Raddatz BW, Kim EYS, Imamura LM, Steil GJ, Santiago EB, Soares SPT, et al. Development of an optimized colorimetric RT-LAMP for SARS-CoV-2 assay with enhanced procedure controls for remote diagnostics. Sci Rep. 2022;12(1):21424.
42. Wu S, Liu X, Ye S, Liu J, Zheng W, Dong X, et al. Colorimetric isothermal nucleic acid detection of SARS-CoV-2 with dye combination. Heliyon. 2021;7(4):e06886.
43. Amaral C, Antunes W, Moe E, Duarte AG, Lima LMP, Santos C, et al. A molecular test based on RT-LAMP for rapid, sensitive and inexpensive colorimetric detection of SARS-CoV-2 in clinical samples. Sci Rep. 2021;11(1):16430.
44. Rossen L, Nørskov P, Holmstrøm K, Rasmussen OF. Inhibition of PCR by components of food samples, microbial diagnostic assays and DNA-extraction solutions. Int J Food Microbiol. 1992;17(1):37–45.
45. Mosolygó T, Laczi K, Spengler G, Burián K. A practical approach for quantitative polymerase chain reaction, the gold standard in microbiological diagnosis. Sci. 2022;4(1):4.
46. Wilson ML, Gaido L. Laboratory diagnosis of urinary tract infections in adult patients.
47. Arunrut N, Jitrakorn S, Tondee B, Saksmerprome V, Kiatpathomchai W. Real-time triplex loop-mediated isothermal amplification (LAMP) using a turbidimeter for detection of shrimp infectious hypodermal and hematopoietic necrosis virus (IHHNV). J Aquat Anim Health. 2024;36(3):205–19.
48. Ptitsyn KG, Khmeleva SA, Kurbatov LK, Timoshenko OS, Suprun EV, Radko SP, et al. Lamp primer designing software: the overview. Biomed Chem Res Methods. 2024;7(4):e00226.
49. Mekata T, Satoh J, Nakayasu C, Ishii Y, Harakawa S, Kawakami H, et al. Development of quantitative real-time PCR and loop-mediated isothermal amplification (LAMP) assays for detection of *Microsporidium seriolae*. Fish Pathol. 2021;56(2):53–61.
50. Khan M, Wang R, Li B, Liu P, Weng Q, Chen Q. Comparative evaluation of the LAMP assay and PCR-based assays for the rapid detection of Alternaria solani. Front Microbiol [Internet]. 2018 Sep 3 [cited 2025 Jul 22];9. Available from: https://doi.org/10.3389/fmicb.2018.02089/full

51. Sakatoku A, Suzuki T, Hatano K, Seki M, Tanaka D, Nakamura S, et al. Inhibitors of LAMP used to detect *Tenacibaculum* sp. strain Pbs-1 associated with black-spot shell disease in Akoya pearl oysters, and additives to reduce the effect of the inhibitors. J Microbiol Methods. 2024;223:106986.

Publisher's Note

Springer Nature remains neutral with regard to jurisdictional claims in published maps and institutional affiliations.